Analysis of Development Methods for Gravel Envelope Wells

E. John List, Ph.D.

E. John List, a native of New Zealand is a graduate of the University of Auckland. In 1965 he was awarded a Ph.D. in Applied Mechanics and Mathematics from the California Institute of Technology. Following a year as a resident fellow at Caltech he returned to the University of Auckland as a senior lecturer in Theoretical and Applied Mechanics. Since 1969 Dr. List has served on the faculty of Caltech in various capacities. Currently he is the professor and executive officer of environmental engineering sciences. His academic interests include hydrodynamics, analysis of pressure transients, and flows through porous media.

Table of Contents

Summary

Five basic techniques of well development have been studied. The purpose of the investigation was to provide a quantitative basis for evaluating the relative efficiency of respective development methods in gravel envelope wells. The techniques evaluated were:

- jetting
- line swabbing
- rocker beam swabbing
- single swab mounted on drill pipe with simultaneous injection below the swab
- double swabs mounted on drill pipe with injection between the swabs

The analysis assumed a completed well with a filter pack between the screen and the aquifer. The primary goal of the studies performed was determination of the direction and magnitude of the flow velocity field at the pack/ formation interface. Evaluation of this flow velocity distribution gives clear indication of the ability of the development techniques to clean drilling debris and wall cake from the formation. Results of the study indicate that both swabbing and jetting can be effective development mehods for gravel envelope wells. Swabbing methods involving pumping appear to offer even further benefits. The efficiency of jetting techniques is found to be conditional on use of a filter pack size distribution that will enable filter particle circulation to develop. In the absence of this circulation, jetting is likely to be of limited use.

Symbol Table

a	well screen radius (ft)
b	borehole radius (ft)
c	jet radius (ins)
D	distance from swab to well bottom (ft)
g	gravitational acceleration (ft/sec^2)
h_1	head loss across leaking swab (ft H_2O)
H	head differences across a swab (ft H_2O)
k_1	hydraulic conductivity of filter pack (gpd/ ft^2)
k_2	hydraulic conductivity of formation (gpd/ ft^2)
2L	swab spacing with double swabs (ft)
Q	injection flow rate (gpm)
R	dimensionless parameter $(\frac{aSU}{2k_1})$
S	specific storativity (ft^{-1})
t	time (sec)
T	thickness of filter pack (ins)
U	velocity of moving swab (ft/ sec)
v_e	tangential velocity of radius b, double flange swab (ft/ sec)
v_j	jet velocity (ft/ sec)
v_o	scaling velocity for double flange swab (ft/ sec)
v_r	radial velocity of radius b (ft/ sec)
v*	scaling velocity for single flange swabbing (ft/ sec)
V	discharge velocity through leaking swab (ft/ sec)
z	distance from swab along well axis (ft)
π	pi = 3.141593

1.0 INTRODUCTION

Constructing of gravel envelope wells by the hydraulic rotary drilling system requires circulation of a drilling fluid in order to remove drilled cuttings from the borehole, lubricate the drill string and bit, provide sufficient hydrostatic pressure to overbalance formation pressures and deposit a thin impervious filter cake on the borehole wall. This mud system along with residual solids remaining in the borehole will reduce well capacity significantly unless removed prior to production.

The process of development first requires that these drilling byproducts be removed from the interface between the borehole and the filter pack in order that final development, which consists of removal of fine materials from the aquifers and stabilization of pack-aquifer materials around the well screen, can be carried out. Preliminary development of gravel envelope wells normally consists of various combinations of circulating, swabbing, jetting, and other methods of conditioning filter pack prior to installation of a turbine development pump.

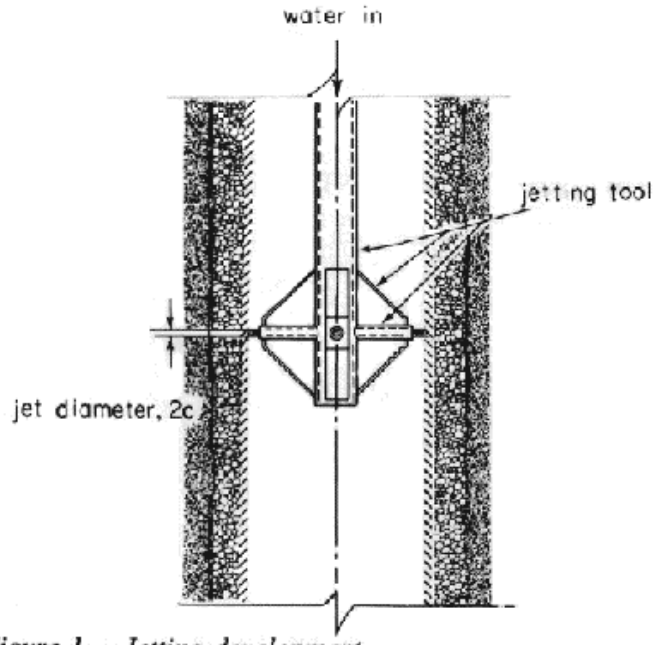

Figure 1. Jetting development

*See References, page 13.

This report provides a scientific basis for evaluation of some of the most commonly used preliminary development methods. It describes in general terms mathematical models of these methods. The results of a laboratory study of a test model of the jetting method will be included. Also included are techniques used in common well configurations. From the results presented it will be concluded that development methods vary considerably in their effect and should be selected carefully to match project requirements.

The five basic methods to be analyzed will be described briefly. The first considered is jet development. As described in The Johnson Driller's Journal, January-February 1979* , this method was developed in an attempt to provide high levels of flow energy to any wall cake on a borehole wall. **Figure 1** shows schematically a typical jetting operation. Typical recommended jet velocities are 150-190 ft/ sec with a jet orifice of ¼ inch to ½ inch.

The second method, line swabbing (**Figure 2**), involves successively raising and lowering a rubber-flanged scow. Typical haul velocities will be on the order of 3 ft/ sec. The scow is equipped with a flapper valve at the foot to facilitate the down motion of the swab.

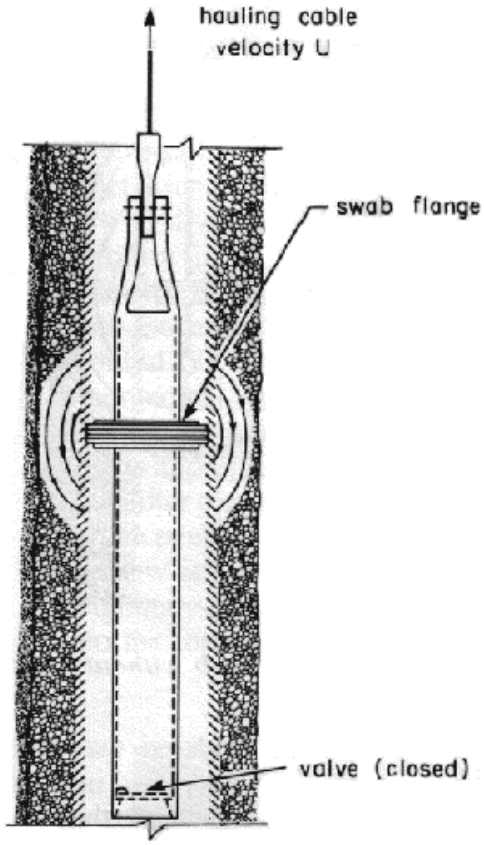

Figure 2. Line swabbing

* See References

The third method, a variation of the previous technique, uses a rocker arm to provide an oscillatory motion of the swab as it is hauled. Typical oscillation will be 30 strokes/ minute with a 3 ft stroke.

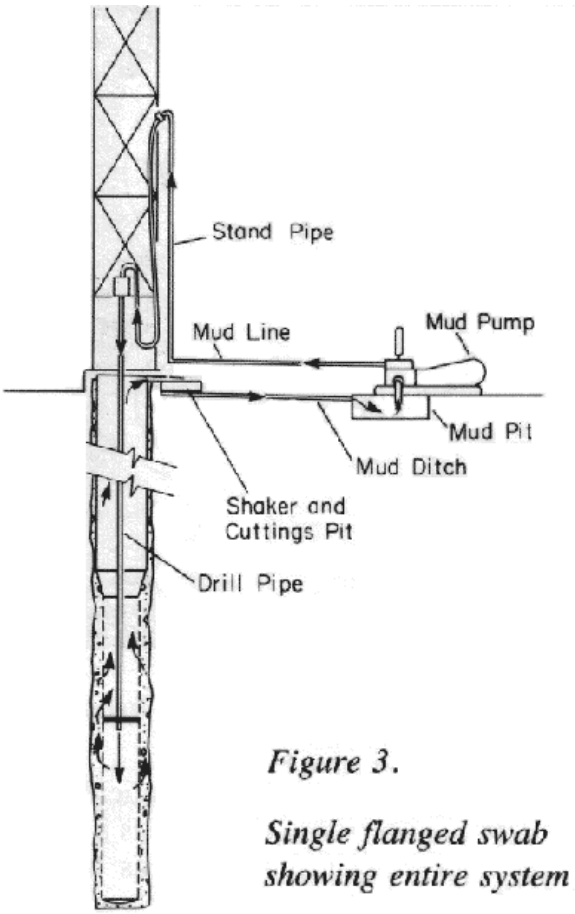

Figure 3.

Single flanged swab showing entire system

The fourth method involves pumping below a single swab mounted on drill pipe so that the swab causes return flow to enter the gravel envelope and bypass the swab, as shown in **Figure 3**. The swab may be hauled and dropped simultaneously with pumping. A typical fall velocity would be 8 ft/ sec.

The fifth method considered uses a double swab mounted on a drill pipe. As depicted in **Figure 4**, fluid is pumped out between the swabs into the gravel envelope. In an alternative version,
the swab is equipped with a bypass to allow flow from below the lower swab to pass to the well region above the upper swab (**Figure 5**).

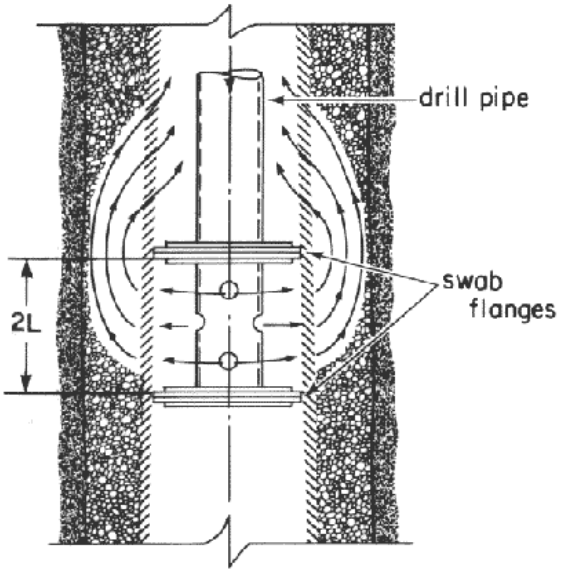

Figure 4. Double flanged swab without bypass

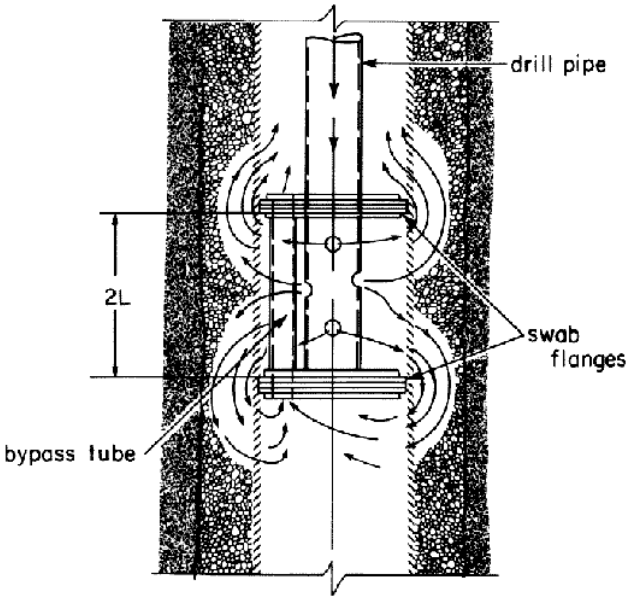

Figure 5. Double flanged swab with bypass

The basic feature of the mathematical models of each of these systems are similar. There is a completed well of radius a, a filter pack of radius b, and assumed hydraulic conductivities in the filter pack and formation of k_1 and k_2 respectively (**Figure 6**). It is assumed that k_1 greatly exceeds k_2. Typical values of k_1 and k_2 are 10,000 gpd/ ft^2 and 100 gpd/ ft^2 respectively, giving a ratio k_2/k_1 of order 0.01. This ratio may vary from 0.1 to 0.001 but, as will be shown, results obtained generally show a great insensitivity to the ratio k_2/k_1.

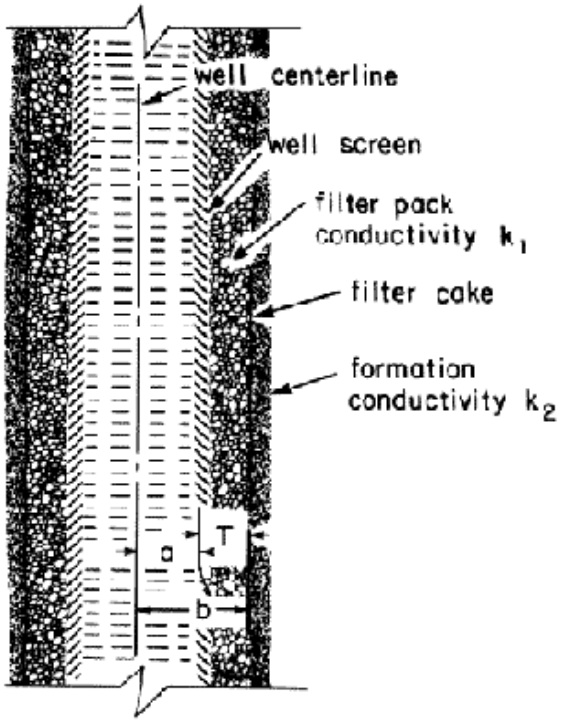

Figure 6. Nomenclature for modeling

The basis for assessment of the development methods will be the magnitude of scouring velocity induced at the filter pack/ formation interface by development flow circulation. This circulation fluid velocity has two components. One is the radial to the well axis, the other tangential or parallel to the well axis. Tangential fluid velocity at the filter pack/ formation interface is primarily responsible for scouring wall cake. The radial component of this velocity removes the material from the well.

This report considers each technique, its model, and results in turn. Conclusions are drawn with respect to the applicability of the results presented and relative usefulness of development methods considered. A comparison of the different techniques is made for typical practical applications.

Details of all mathematical models are given in **Appendix A**.

2.0 WELL DEVELOPMENT MODELS

Basic models for each of the five well development techniques and computational results from the models are presented in this section.

2.1 Jetting

The purpose of jetting is to provide a high energy flow through the filter pack to the wall cake at the formation. This is considered to occur either by flow through the motionless pack or by physical displacement of the pack material by the jet. Mathematical modeling of either mode of operation is difficult. In the first case, even though it is assumed that the pack will not move, the flow will not obey the Darcy equations for flow in porous media. In these equations velocity is directly proportional to pressure gradient. However, for very strong pressure gradients, the velocity produced is less than would be predicted by the Darcy equations. This implies that their use here will give a favorable representation of the jetting flow.

In the second case, where filter pack is presumed to be displaced by the jet and move with the flow, equations describing the motion of the combined pack-fluid motion are extraordinarily difficult to solve. Furthermore, it is not clear how to predict the boundary that will form between the pack material that moves and that which does not. It is apparent that any evaluation of this mode of jetting action must be performed through use of a laboratory test model.

In the following mathematical analysis it is assumed first that the pack material does not move and that any flushing of the wall cake must occur solely by jet flow. A mathematical model of this operation is developed and its efficiency evaluated. Subsequently, a laboratory test model will be described. This

model has been used to determine when the jet does move the pack material, and provides visual evidence of the mechanisms involved. Each model will be discussed in turn.

2.1.1 Mathematical model of jetting

For the mathematical, the Darcy equations are used to consider a flow field generated in a porous medium by injecting a flow Q over a circular surface of radius c. This is a favorable representation of a jet since, with any high speed jet, a significant fraction of flow would bounce from the screen and filter pack.

The well wall is modeled as a filter pack of hydraulic conductivity k_1 and thickness T (which is equal to the difference in the screen and filter pack radii) and a formation of hydraulic conductivity k_2. In actuality the surface of the formation may well have a hydraulic conductivity much less than k_2 as a consequence of drilling wall cake. The physical configuration is as shown in **Figures 1** and **6**.

Mathematically, this problem is identical to finding the flow of heat into a layered medium, with heat being applied over a circular area of radius c and the surrounding medium being kept at a constant reference temperature. The solution is given for a homogeneous medium (no layers) by Carslaw and Jaeger* (1959), and this serves as a starting point for the solution of the problem with two layers of different conductivity. Details of the solution are given in **Appendix A**. It is in the form of an integral and involves the ration of filter pack thickness to jet radius (T/c), velocity of the jet v_j, distance from the jet impact point on the screen, and the ratio of the hydraulic conductivities of the formation and filter pack. Numerical evaluation of the solution is possible using a digital computer so that flow fields can drawn in both the filter pack and formation.

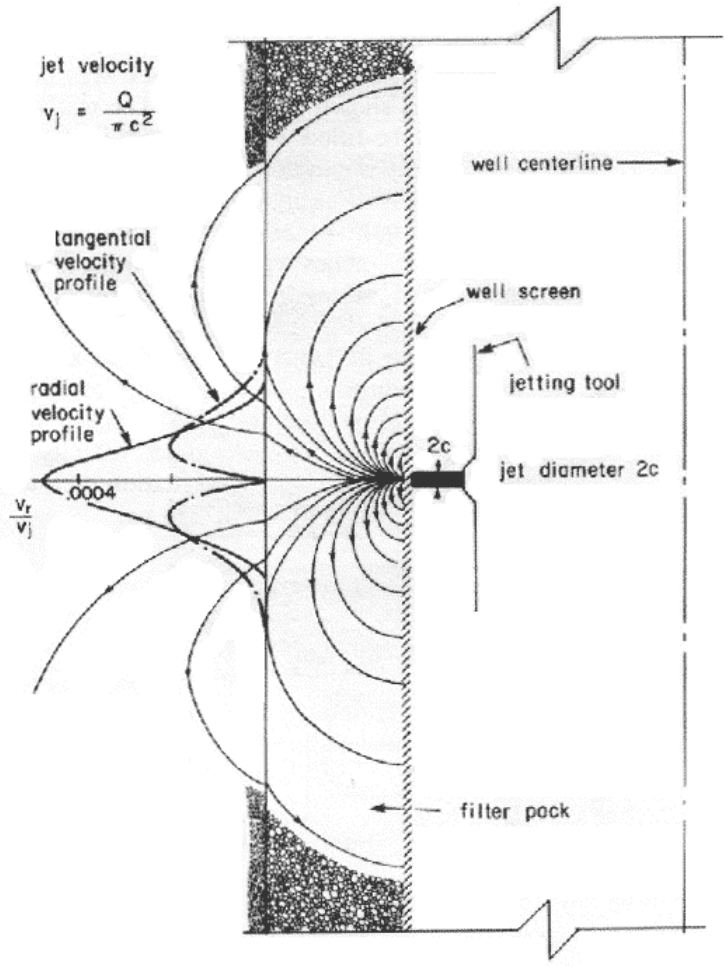

Figure 7. Radial and tangential velocities produced within filter pack by jetting development with no filter pack movement and T/c = 12

Figure 7 shows graphs of radial and tangential velocities into and along the formation/ filter pack interface for the case when ratio of jet radius to filter pack thickness is 1 to 12 (e.g., ½-inch diameter jet into 3-inch filter pack). Velocities are given as a fraction of jet discharge velocity v_j, where v_j is the jet flow Q divided by jet area πc^2. Pak radial velocity into the formation is less than 1/2000th of the original jet velocity v_j and peak tangential velocity along the formation is only 1/5000th of the original jet velocity. In other words, very little jet energy propagates into the formation. This is confirmed by the results appropriate to the problem when there is no filter pack. In this case, an exact solution for the peak radial velocity can be found (see Carslaw and Jaeger, 1959) and it indicates a magnitude of the order $(c/T)^3 v_j$ at depth T into the formation when c/T is small.

When the ratio of filter pack thickness to jet radius is 28 (7-inch filter pack and ½-inch diameter jet), velocities are even lower. Computations show a peak tangential velocity at the interface of the

filter pack and formation of only 1/59000th of the jet velocity.

The results make it clear that very little jet flow energy will penetrate more than a few jet diameters into the filter pack, and very little flow will be generated at the filter pack/ formation interface. Recall that this solution was based on Darcy flow equations and a presumption that all jet flow would enter the filter pack. Given that, at high jet flow velocities, friction will be greater and a fraction of the jet flow will bounce off the
well screen and filter pack, the induced velocities will be lower than those predicted in the above analysis. The above results are, of course, only valid when the integrity of the filter pack is maintained. In the event of disruption of the pack to a degree that the jet directly impacts the formation, these conclusions no longer will be valid, and
recourse is made to a laboratory test model.

* See References

2.1.2 Laboratory model of jetting

A laboratory test model of a section of a well with an artificial filter pack was constructed as shown in **Figure 8**. The test section could be filled with a selected pack, the top and diaphragm bolted own and an overburden pressure as high as 60 psi imposed via the diaphragm. A test jet with internal diameter 0.167 inches was located in the model such that the flow from the jet directly impacted the section of well screen. The distance of the jet from the screen was adjustable, allowing simulation of a jet of larger diameter. Maximum jet flow possible was 12 gpm, corresponding to a jet velocity of close to 180 ft/ sec and a stagnation pressure within the gravel of about 220 psi.

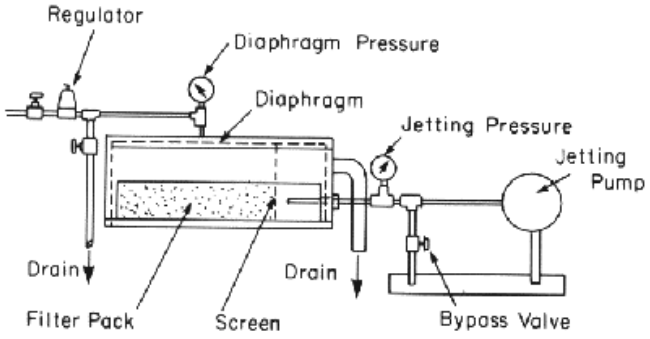

Figure 8. Laboratory jetting model

The purpose of this test facility was to determine the mode of jet operation and evaluate the influences of pack material size distribution, jet flow rate, and overburden pressure on the jetting operation. Tests were performed with three pack material sizes commonly employed in gravel envelope wells. Details of the materials are given in **Appendix B**. The well screen used was the continuous wire wrap type, constructed with 0.060 inch aperture size.

The fundamental result of the tests performed shows that pack material will not move under jet action unless there is sufficient free space in the filter pack. In other words, there must be "elbow room" for the particles. In the tests this could be provided either by release of the pressuring diaphragm or by waiting for the jet to wash enough fine particles through the screen to create the space. No motion occurred in the test using 1/8 1/4 gravel filter pack (**Appendix B**).

Operation of the test apparatus with finer pack material, such as a 6 14 Crystal Silica gravel (**Appendix B**), disclosed that pack motion would develop only after a cavity was formed by elutriation of the finer size fraction of pack material through the screen. The progression of the pack motion was systematic. First, a few grains would move in the initial cavity formed. The motion of these grains in turn allowed the jet to penetrate deeper and was out more fine material, thereby increasing the free space. The flow of jet fluid and pack material developed a vortex structure which advanced into the filter pack until an equilibrium penetration depth was attained in about two minutes (**Figure 9**).

At equilibrium it appears that total jet power is consumed in keeping a ball of fluid and pack material in motion, and none is available to generate new particle motion. It is to be expected that reducing the intergranular stress in the motionless pack should allow the depth of penetration of the jet to increase. This argument is confirmed in the test results. In **Figures 10** and **11** overburden pressure, as

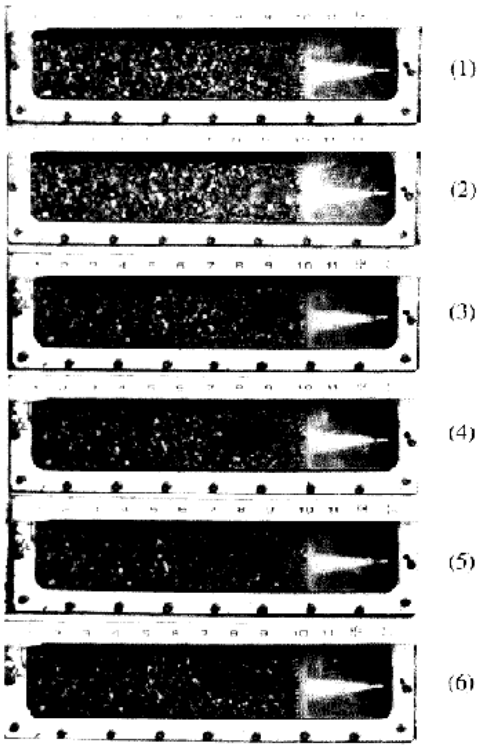

Figure 10. Sequence of photographs showing further development of whorling Crystal Silica gravel/fluid motion following release of overburden pressure. Photograph timing is according to:
(1) 45:52 (3) 47:03 (5) 47:19
(2) 46:53 (4) 47:13 (6) 47:27

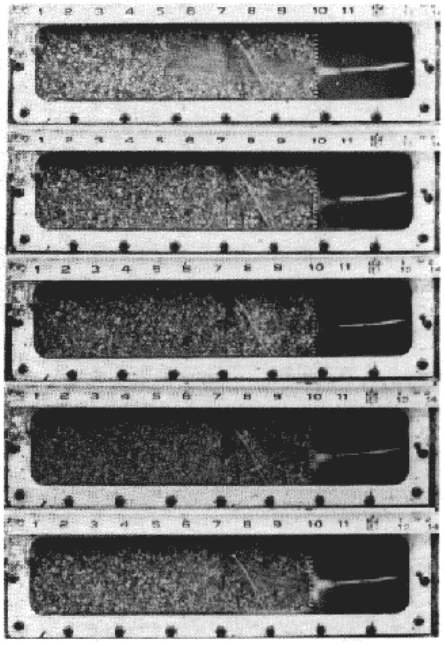

Figure 11. Sequence of photographs showing lock up of Crystal Silica gravel subsequent to jet pressure reduction. Photographs in sequence are:

Time	*Jet Velocity*
(1) 51:48	*170 ft/sec*
(2) 53:33	*100 ft/sec*
(3) 53:50	*130 ft/sec*
(4) 54:46	*150 ft/sec*
(5) 55:15	*180 ft/sec*

represented by the test cell diaphragm, has been released, thus providing more free volume and a reduction in the intergranular stress. The result is an increase in jet penetration from about 2 ½ inches to 4 ½ inches.

Results depicted in **Figures 9**,**10** and **11** are typical of all the test results with both 6 10 and 6 14 sands. Initial development of motion depends upon either the existence or creation of free space in which particles of pack material can move. Once particles are free to move, the scale of motion depends upon jet velocity, overburden pressure, the degree of compaction of the filter pack, and intergranular friction. The influence of each of these factors was apparent in the tests.

Considering only the effect of jet velocity, it was clear that reduction in flow velocity reduced the depth of penetration once the system was in motion. A second increase in jet velocity would not generate penetration depth equal to that attained initially, a somewhat surprising result. The explanation lies in the greater degree of compaction attained in the pack material by the jetting action over what was initially present. This phenomenon is illustrated in **Figure 11**. This was also confirmed in another test, in which the overburden pressure was suddenly released to allow the filter pack material to move. The whirling mass of fluid and filter pack subsided to about half of its initial extent as the pack material compacted. In general, penetration depth attained with a smooth rounded sand (6 10) appeared to be marginally greater than that with a sharp angular sand (6 14).

All tests were performed with a 0.167 inch diameter jet. In order to simulate the effect of a larger diameter jet, the jet, originally ¾ inch from the screen, was moved back to provide a larger impact area. This test, which was performed on a gravel pack that had been in motion, indicated that the effect of the jet impact area was not significant. As can be seen in **Figure 12**, where the jet is 20 diameters from the screen, motion of the pack material and depth of penetration increased as overburden pressure was released. This result confirms that it is jet power which controls the dimension of the filter pack movement and not jet diameter.

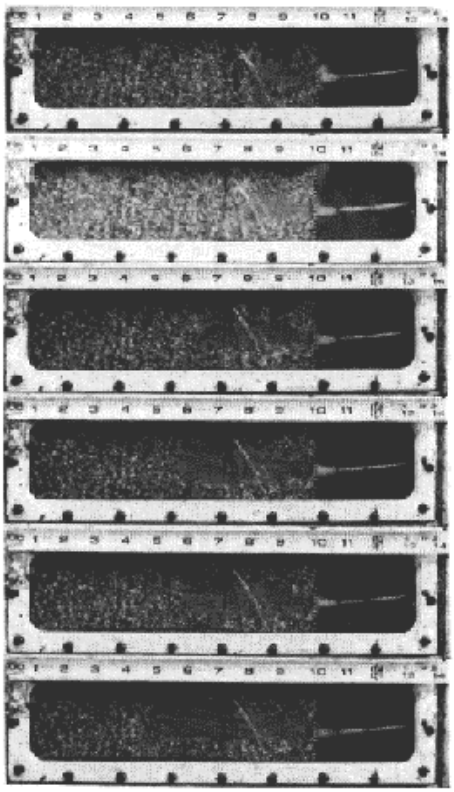

Figure 12. Sequence of photographs showing motion in 6 x 10 rounded gravel produced by a jet located 20 jet diameters from the well screen. Gravel has been previously in motion brought about by production of a cavity as in Figure 9. Note jet cavitation at high flow velocity. Photograph sequence is:

(1) 48:06	*Overburden pressure 30 psi*
(2) 48:14	*Overburden pressure 20 psi*
(3) 48:19	*Overburden pressure 15 psi*
(4) 48:24	*Overburden pressure 10 psi*
(5) 48:29	*Overburden pressure 5 psi*
(6) 48:45	*Overburden pressure 0 psi*

To summarize, the key element in getting pack material into motion is the ability of the jet to create moving space by washing out fine materials from the filter pack in progressive fashion described If the filter pack is compacted, and of a size distribution that none will pass through the well screen, it appears no motion is possible. Once the pack material is in motion it can be sustained with lower velocities than are required to initiate motion. The size of the moving region is a function of the power available in the jet relative to the power necessary to keep a given volume of fluid and pack material in motion. The relationship of these conclusions to actual well development will be reviewed in Section 3. No discussion is presented here of the potential deleterious effects of creating filter pack cavities. This consideration, however, is important in filter pack selection when jetting development methods are to be used.

2.2 Development by Line Swabbing

Line swabbing is the term given to hauling a close fitting rubber flanged scow through the well. As shown in **Figure 2**, its purpose is to develop a pressure differential across the section of well containing the swab. This pressure differential results in flow being forced into the well screen on the high pressure side and out of the screen on the low pressure side. Because the scow is equipped with a foot valve, it drops easily and the process can be repeated.

Modeling the flows developed by this process must be done in two stages. First there is radial production flow generated by placing the swab in motion. This is accompanied by a steady state motion about the swab when seen from coordinates moving with the swab. We look at each of these separately, since analysis of the system over the complete range of motion is very difficult.

Consider the swab at rest with the well at equilibrium. Moving the swab upwards causes the well to flow at a rate that matches the flow generated by the swab. If there is D feet of screen below the swab, then at the filter pack/formation interface radius b (and assuming no leakage past the swab) we must have a radial inflow velocity v_r given by

2π b $Dv_r = \pi a^2 U$

so that the inflow velocity is

$$v_r = \frac{a^2 U}{2bD} \qquad (1)$$

where a is the radius of the well U is the velocity of the swab.

This radial velocity will gradually decrease as D increases due to the rising swab. It is conceivable that the aquifer may not produce flow at the rate induced. If not, then pressure in the well below the swab will continue to drop and may even reach vapor pressure, forming a vapor cavity behind the swab. The magnitude of pressure drop is controlled by the productive capability of the aquifer, leakage past the swab and bypass flow through the filter pack about the swab. This pressure drop will gradually decrease with time since more well surface area capable of producing is exposed as the swab rises. Maximum well production clearly cannot exceed the equivalent flow produced by the swab motion, so that a maximum value for the production velocity component is that given above in equation (1).

The pressure rise above the swab as the swab lifts water in the well above the static point will continue to increase until limited by one of two effects. The well will overflow as water reaches the surface, or a level will be attained where the head is sufficient to cause flow into the aquifer and bypass around the swab at a rate that exactly matches the flow produced by the swab motion. This bypass through the filter pack will flush drilling debris and wall cake from the filter pack/ formation interface and deposit it in the well behind the swab. Swab-induced flow can be modeled mathematically by ignoring the top and bottom aquifer boundaries and by considering the flow in a system of coordinates moving with the swab. Basic parameters controlling the solution are the ratio of filter pack to well radii b/a, ratio of hydraulic conductivities k_2/k_1, and the distance up or down the well from the swab in terms of well radii (z/a). Results are given in terms of multiples of a scaling velocity v* which is defined by

$V^* = k_1 H / \pi a \qquad (2)$

where H is the head difference across the swab
k_1 is the hydraulic conductivity of the filter pack
a is the well radius

Speed of the swab enters the problem in two ways. As noted above, it controls the magnitude of the head difference across the swab. It also enters in the form of a dimensionless parameter

$R = aSU / 2k_1$

where U is swab velocity
S is the specific storativity of the filter pack

In general, S is small* so that the parameter R will usually be in the range of 0.1 - 0.001. In the particular case when R = 0.1 and the ratio of filter pack radius to well radius is 1.5, distribution of tangential (along the well) velocity at the formation/ filter pack interface is given in **Figure 13**. Peak tangential velocity at the interface of the formation and pack is found to be 2.9 v*.

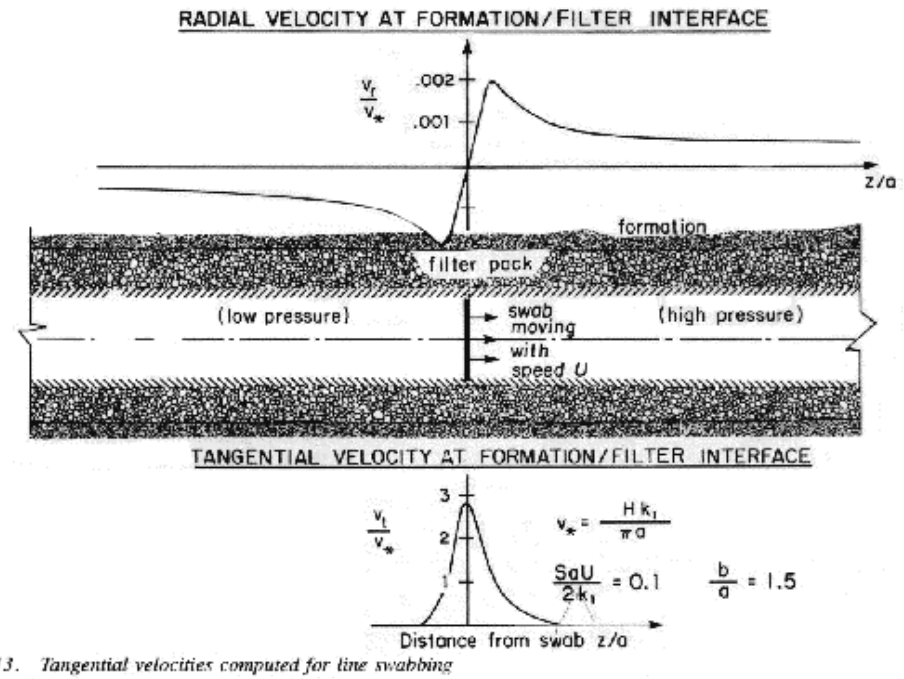

Figure 13. Tangential velocities computed for line swabbing

In the case when $R = aSU/2k_1 = 0.001$, the magnitude of the peak tangential velocity at the interface increases slightly to 3.0 v*. The solution appears to be relatively insensitive to R in the range of practical interest.

The results above were developed relative to a coordinate frame moving with the swab. To reduce these results to a fixed reference frame, the variable z, the distance from the swab, must be replaced by z - Ut. This means that at a fixed point in the well the velocity experienced will be similar to that shown in **Figure 13** as if the well axis were time. Tangential velocity at the formation/ filter pack interface will be experienced for a time of approximately 2a/U, which will be relatively short for common well sizes and swabbing speeds.

Radial velocity is also developed by the swab bypass flow. There will be flow into the formation ahead of the moving swab, and flow out of the formation behind it. This flow velocity is also scaled by v*, and a graph of radial velocity, v_r/v^*, as a function of distance ahead of and behind the swab is given in **Figure 13**. The magnitude of this radial velocity will not be high, relative to the peak tangential component of velocity along the well. Nevertheless, behind the swab it will form a steady inflow into the well which will carry drilling debris along with it.

In summary, line swabbing is a two-stage process involving production inflow generated by the swan displacement followed by high velocity tangential motion in the filter pack coupled with a more uniform radial well inflow. Repeated applications of the process will be effective in clearing drilling debris and wall cake from the borehole.

2.3 Rocker Beam Swabbing

In this method, of well development the swab is oscillated up and down in the screen section. The exact modeling of this technique is extraordinarily difficult. The problems arise from having to satisfy a condition on the swab surface that is being accelerated then decelerated continuously. In the previous case a simple change in coordinates was sufficient to enable a solution to be found. Here we look for a solution that has a periodic nature, with frequency f (circular frequency $\omega = 2\pi f$). The results (**Appendix A**) involve numerical computations that are very time-consuming even with a digital computer. However, a simplification is possible by noting that the basic parameter of the solution is $a^2 \omega S / k_1$. This has a very small magnitude and the solution is equivalent to a motionless swab with a steady pressure drop across it. The oscillatory solution therefore is of the form of this steady state solution multiplied by cos ω t.

Computations of the solution obtained in this way gives the tangential velocity distribution presented in **Figure 14**. This figure includes a schematic of the flow field expected in the filter pack. It is interesting to note that, for a short swabbing stroke, results obtained for $k_2/k_1 = 0.001$ and b/a = 1.5 give a tangential velocity ratio $v_t/v^* = 3.0$, agreeing well with results obtained for line swabbing, even though separate methods were employed. This is a satisfying check on the computation.

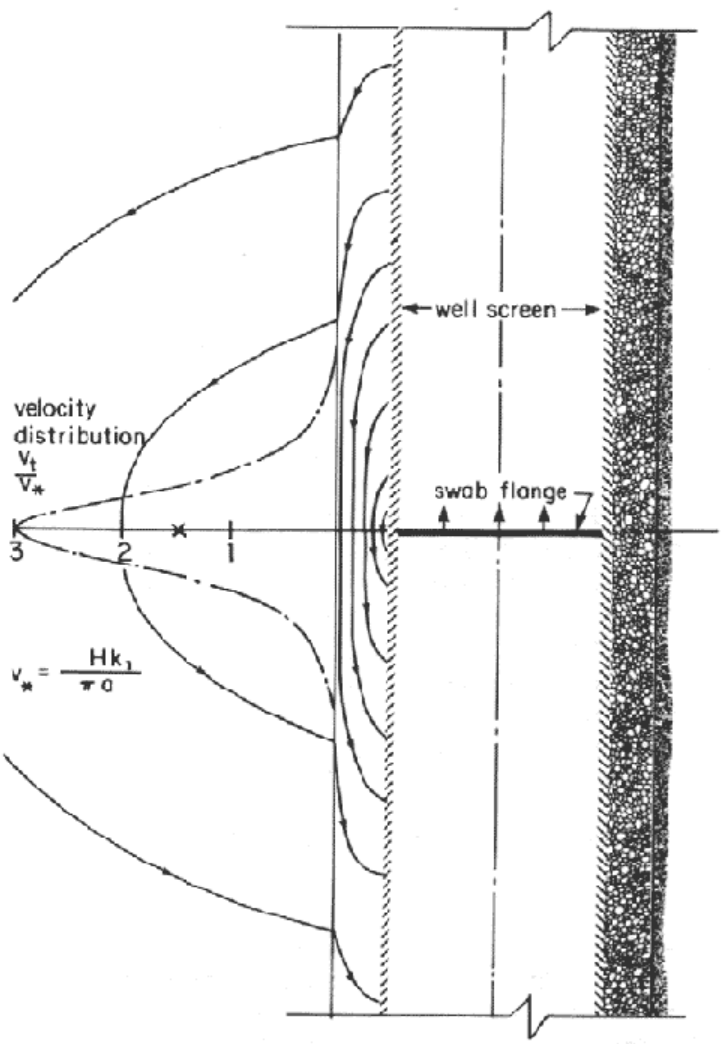

Figure 14. Peak tangential velocities computed for rocker beam swabbing

For b/a = 2.0 the peak velocity is reduced to 1.5 v*, or 50% of that for b/a = 1.5. (See point X in **Figure 14**.) The solution shown in **Figure 14** represents peak velocities to be expected from rocker beam swabbing. This would be repeated with each uphaul of the beam. Complete reversal will not occur because of the foot valve. Peak radial velocities induced by the swab motion are shown in **Figure 13**. These are also cyclic with the swab motion.

2.4 Single Swab Mounted on Drill Pipe With Simultaneous Injection Pumping Below the Swab

In this method of development, flow is injected into the well below a swab-equipped drill pipe (**Figure 3**). The injected flow must bypass the swab through the gravel envelope or enter the formation. The mathematical model for this operation is almost identical to that for line swabbing but with the pressure drop reversed. Head provided by the pump at the surface will control head difference across the swab when the swab is stationary.

There is a basic difference from line swabbing. Sections of the well above and below the swab will be subjected to a pressure excess over the original static pressure in the well. Consequently, the well will act as a recharge well.

Recharge potential of the well will be controlled by the hydraulic conductivity of the wall cake and increase in static pressure. For a given head drop across the swab the effect of this recharge will not modify the magnitude of the tangential velocity profile because recharge flow is always radial. There remains the question, of course, of how much head is used in radial flow and how much is used to flush

the filter pack. It seems reasonable to assume that the head difference between the pumping head and overflow is used for flushing and head difference between the overflow and the original static for recharge. The line swab results in **Figure 14** utilizing the head difference between the overflow and pumping levels minus the head losses in the delivery pipe are used to determine the flushing velocities.

If the swab is placed in motion by hauling the drill pipe then some modification of the previous analysis is required. On an up motion of the swab the tangential velocity in the filter pack will be reduced and may come to zero. The latter occurs when the speed of the haul, multiplied by the area of the swab, exactly matches the flow delivered by the pump. On the down stroke flushing effectiveness is enhanced since the effective flow rate will be that delivered by the pump added to that induced by the swab motion. A numerical comparison of the two cases is made in section 3.

2.5 Double Swabs Mounted on Drill Pipe With Simultaneous Injection Pumping Below the Swab

In this method of development, flow is injected into the filter pack from between two adjacent swabs (**Figure 4**). A flow Q is forced into the filter pack and reenters the well above and below the swabs. There is a variation of this method which incorporates a bypass connecting the sections of well above and below the swabs.

Consider the first case without a bypass. Flow forced into the filter pack has two routes. It moves upward, reenters the well and flows to the surface, or it moves downward to the lower section of the well and must flow into the formation as recharge. In both cases, it must pass through the filter pack.

If the formation has any resistance to recharge, the section below the swabs will be pressurized very quickly and flow will pass upward through the filter pack to the surface. The net result will be similar to that described in section 2.4. Peak tangential velocities will be given by the pumping head, corresponding to injection with a single swab, as shown in **Figures 13** and **14**.

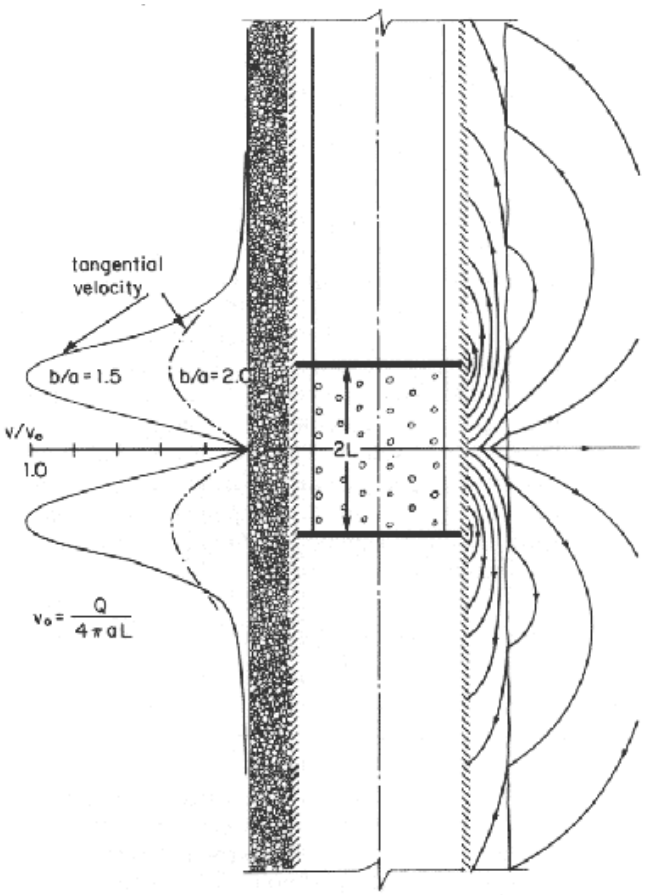

Figure 15. Radial and tangential velocities obtained from mathematical model of double flange swabbing

If there is a flow bypass from the lower section of well to the upper section, the flow configuration is different. Flow will move in both directions within the filter pack, and even if significant recharge occurs in the well all flow must exit between the swabs via the filter pack. Geometry for the mathematical model and numerical results obtained from the model described below are depicted in **Figure 15**. The scaling velocity in this case is

$$v_0 = \frac{Q}{4\pi a L}, \qquad (4)$$

which is the mean velocity for flow exiting between the swabs. For swabs spaced a distance equal tot he well diameter, peak tangential velocity at the filter pack/ formation interface is found to be equal to v_0 when b/a = 1.5, as shown in **Figure 15**. When b/a is increased to 2.0 peak tangential velocity drops to 0.36 v_0, as shown by the dotted curves in **Figure 15**.

Peak tangential velocity appears to depend rather weakly on the ratio of k_2/k_1 (the hydraulic conductivity ratio). Changing k_2/k_1 from 0.001 to

0.1 reduces peak tangential velocity by about 10%, because more flow will leak into the formation

Radial velocities are also induced by the pumping operation. There is a weak inflow into the formation, adjacent to the swabs, as depicted by the streamlines in **Figure 15**. This flow reverses to become a flow out of the formation within a distance from the swabs about equal to half the swab spacing. The magnitude of these velocities is small relative to the tangential velocities in the filter pack and probably does not contribute much toward flushing.

For this case it is possible to estimate the magnitude of the tangential velocity at the filter pack/ formation interface. If we assume that the flow out between the swabs divides equally into an upflow and a downflow, and that vertical velocity distribution in the filter pack is uniform, then the estimated tangential velocity v_e is given by

$$\pi(b^2 - a^2)\, v_e = Q/2 \qquad (5)$$

since all flow must pass through the annular area comprising the gravel envelope. From equations (4) and (5) it is possible to show that

$$\frac{a v_e}{L v_0} = \frac{2}{(b/a)^2 - 1} \qquad (6)$$

This relationship is presented in **Figure 16** jointly with the tangential velocity to scaling velocity ratio as derived from the mathematical model given in **Appendix A**. **Figure 16** demonstrates that the dependence of the mathematically predicted tangential velocity on the ratios of b/a and L/a is very close to that estimated in equation (6) above. However, peak tangential velocities are found to be less than the estimated values. This can be ascribed to non-uniformity in the velocity distribution, as is apparent from the fact that the mathematically predicted value becomes a smaller fraction of the estimate as b/a increases except for increasing L/a.

Results in **Figure 16** can therefore be used to evaluate peak tangential velocities for any practical ratio of b/a and L/a.

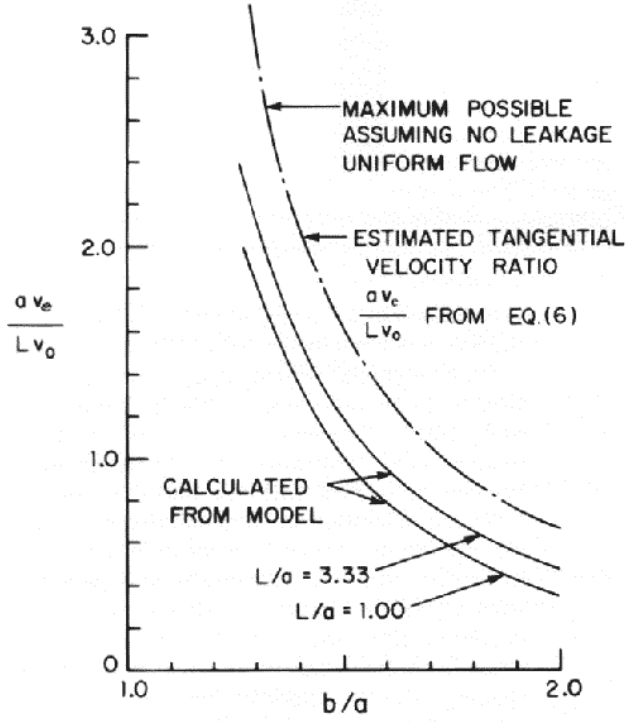

Figure 16. Flushing velocities for double flange swabbing with a bypass, given as a function of L/a and b/a as computed by the mathematicial model. Also shown is the estimate based on uniform flow in the filter pack.

3.0 COMPARISON OF DEVELOPMENT METHODS

In this section we compare the methods as applied to a 14-inch diameter well with 7-inch filter pack, giving a dimensional ratio b/a = 2.0. Hydraulic conductivity of the filter pack is assumed to be 10000 gpd/ ft^2 and the formation 100 gpd/ ft^2, giving a ratio $k_2/k_1 = 0.01$, which is within the range used in the computations. We consider each development method in turn.

3.1 Jetting Development

Consider first a well with filter pack particle size distribution that does not permit any filter pack material to pass through the screen, restricting pack motion. In this case assume three jets each ½-inch in diameter and operating at 104 gpm at 250 psi, providing jet velocity of 190 ft/sec (Zdener and Allred 1979). The ratio T/c = 28. Using formulae given in **Appendix A**, the peak tangential velocity at the filter pack/ formation interface cannot exceed 0.003 ft/sec.

Jet development is essentially useless in this configuration. Results indicate that for any practical thickness of filter pack (>2 inches) in a situation where pack motion is impossible, jet development is inappropriate since velocities generated at the interface of the filter pack and formation are too small to be of much use.

Now consider the situation where gravel motion can be initiated by creation of a cavity through elutriation of finer material. In this case flow patterns will be established such as shown in the photographs of **Figures 9**,**10**,**11** and **12**. The question is how will the flow fields vary with jet diameter and jet flow. The answer is relatively simple. Power in the jet is proportional to the product of the discharge rate Q and velocity v_j, or, writing this in terms of jet diameter 2c and jet velocity v_j, jet power is proportional to . Power dissipation in the motion of pack material will be proportional to and to the volume of material placed in motion. Thus, for given jet flow velocity and pack material it would be expected that the volume of gravel in motion will be proportional to c^2, everything else held constant. The linear dimension of volume in motion should then increase as $c^{2/3}$. Given a jet 0.167 inches in diameter, delivering water at 180 ft/sec, with a volume of moving pack material 5 inches deep, then a jet 0.5 inches in diameter delivering water at about the same velocity should produce a moving pack volume about 10 inches deep, provided free volume for material to move either exists or can be created by flushing fine material through the screen. The fact that this may not always occur helps explain mixed field results using this method of development.

If the filter pack can be placed in motion by the jet, effective flushing will develop. Motion of the jetting tool must necessarily be slow or there is a strong probability of moving the jet away from the pack material in motion. In regions with high over-burden pressures giving high intergranular stress, development of pack motion will be very slow and the technique less effective. With low intergranular stress and excessive fine filter material, slow jet motion may destroy effectiveness of the filterpack through the creation of cavities.

3.2 Line Swabbing

In the swabbing analysis performed in Section 2.2, it was explained that the process occurs in two stages. First, there is a radial flow velocity at the borehole of

$$v_r = \frac{a^2 U}{2bD} \qquad (7)$$

where a is the well radius
U is swab velocity

b is filter pack radius
D is depth of well screen below the swab

Second, a tangential velocity through the filter pack adjacent to the swab is set up. A scale velocity for this process was defined, where

$$v^* = Hk_1/\pi a \qquad (8)$$

where H is the head drop across the swab
k_1 is the filter pack conductivity

The peak tangential velocity v_t was found to be

$v_t = 3.0v^*$ when b/a = 1.5
$v_t = 1.5\ v^*$ when b/a = 2.0

Applying these results to the example of a 14-inch well and 7-inch thick filter pack implies for a swab speed of 3 ft/sec the initial radial velocity at the filter pack/ formation interface will be

$v_r = 0.44/D.$

When the swab is moving near the bottom of the well screen this velocity will be high. With 100 ft of screen below the swab it will be 0.0044 ft/ sec.

In the second stage, with b/a = 2.0, k_1 = 10,000 gpd/ft^2 = 0.0154 ft/ sec we have the tangential velocity

$$v_t = \frac{1.5 \times 0.0154 \times H}{\pi(7/12)} = 0.0126H. \qquad (9)$$

Thus a head difference of 1 ft across the swab will produce four times the tangential velocity at the exterior of the filter pack, as would a ½-inch jet at 190 ft/sec. With a head difference of 10 ft the tangential velocity would be 1.5 inches/ sec. The head H, in effect, is controlled by swabbing speed since, as noted, if the swab is moving fast enough, flow produced will exceed the capacity of the well to absorb it. Actual tangential velocity also depends upon the length of screen above and below the swab and how tightly the swab fits, since these control H, the head available.

The radial bypass flow produced by the swab motion is given in **Figure 13**. Results show that at 50 well radii below the swab there is an inflow velocity at the filter pack/ formation interface of the order of 10-4v*. This must be added to the radial production component induced by the swab but, as can be seen from the previous discussion, it is small in comparison and therefore probably does not play much of a role in the flushing process.

Speculation can arise as to how modifying the diameter of the swab to provide clearance will modify swabbing efficiency. Assuming swab clearance acts as an orifice, head loss across this orifice satisfies an equation of the form

$$h_1 = kV^2/2g \qquad (10)$$

where V is the discharge velocity through the orifice. If V is large, then h_1 may exceed the head required to drive the flow through the filter pack and a reasonable velocity may still be attained within the filter pack. The key issue is whether head loss across the swab clearance is enough to divert flow through the

filter pack. For the case considered above, with a 14-inch well and a 7-inch-thick filter pack, a head of 10 feet would give peak tangential velocities in the pack of 1.5 inches/ sec. A swab with ¼-inch clearance provides a clearance area of 11 square inches. Assuming a head loss coefficient 2 for the orifice, a velocity of 18 ft/ sec is calculated. Thus a flow of about 600 gpm could pass the swab at the head difference necessary to produce tangential velocities in the filter pack of 1.5 inches/ sec.

3.3 Rocker Beam Swabbing

As noted in Section 2.3, peak velocities obtained are, for the same head across the swab, equal to those for line swabbing. However, the effect of the valve in the swab, which allows it to fall back, results in a reduction in the head available to produce a flow through the filter pack. The effect of the rocker beam motion is to "pulsate" the flow in the filter pack. Although head difference available may be reduced by valve action, accelerations associated with the oscillatory motion would provide an excess difference equal to a modification of the gravitational acceleration. A 3 ft stroke and period of 2 seconds results in a peak acceleration of 1.5 π^2 = 14.8 ft/ sec^2, or about g/2. Thus peak tangential velocity through the filter pack is increased by about 50%.

As with the line swabbing the radial effect can be split into a component representing production and a component representing swab bypass flow through the filter pack. Radial flow induced by the production component is governed by the depth of well screen below the swab and peak swab velocity. Peak swab velocity for a 3 ft stroke and period of 2 seconds is 1.5 π ft/sec or about 4.7 ft/sec. Given equal heads, radial velocities are about 50% greater than for line swabbing. Flows are repeated every two seconds so there will be steady migration of particles through the well screen.

Given the pulsating character of flow fields produced by rocker beam swabbing it is probably an effective development tool both for flushing of drilling debris and wall cake and consolidation of the filter pack.

3.4 Single Swab Mounted on Drill Pipe With Injection Pumping Below the Swab

As stated in Section 2.4, peak tangential velocity at the formation/filter pack interface for a stationary swab is equal to three times the scaling velocity v* defined by $Hk_1/\pi a$. The pumping head provides bypass flow, while increase in static head develops a recharge flow. Allowance must be made for the pumping head used to overcome pipe friction.

Suppose a tangential velocity of 1.5 inches/second is considered adequate at the filter pack/formation interface. For a 14-inch diameter well and 7-inch filter pack this is accomplished with a head difference of 10 feet across the swab. Flow that must be delivered to attain this head difference depends on total screen length. Since the entire open well screen is available for recharge, flow to be delivered is controlled by total screen length and formation recharge capability. In any situation the operator can easily ascertain what is occurring from observation of pumping pressure and volume of makeup water required.

Swab motion produced by hauling and dropping the drill pipe creates significant velocities in the filter pack. A typical fall velocity is about 8 ft/ sec. With 14-inch diameter well screen this produces a flow of 3800 gpm, which is generally in excess of injection pumping capacity. Without swab clearance this flow must either be forced into the formation or bypass the swab through the screen. Such flows forced into the filter pack will almost certainly fluidize it and be very effective in scouring wall cake from the borehole. However, if there is considerable screen below the swab, some flow could go into the formation as temporary recharge.

3.5 Double Swabs Mounted on Drill Pipe With Injection Pumping Between Swabs

Without a bypass through the swabs the system acts as a single swab, or can be considered as one half of a bypass-equipped double swab. The analysis is therefore subject to a degree of uncertainty in that some flow will enter the formation as recharge. Hauling and dropping the swab creates the same flows as a single swab. In an example illustrating this development method, 2200 gpm of flushing water was pumped into a newly constructed well with 18-inch diameter casing and 30-inch diameter filter pack. Water was pumped out between double swabs which in one case were spaced 5 ft apart and in another case 18 inches apart. Peak tangential velocity in both cases is approximately the same since, as we have seen, the ratio b/a is the predominantly controlling mechanism. If we assume all flow passes upward through the filter pack and there is essentially no recharge, then tangential velocity cannot exceed

$$v_e = Q/\pi(b^2 - a^2)$$

$$= \frac{2200 / 449}{\pi[(1.5)^2 - (0.75)^2]}$$

$$= 0.93 \text{ ft/ sec.}$$

As shown, actual tangential velocities are, for b/a = 1.7, about 70% of this estimate, giving tangential velocity of about 0.65 ft/ sec. Swab spacing will not influence this significantly.

When there is a flow bypass as described in Section 2.5, and when b/a = 1.5, peak tangential velocity at the formation/ filter pack interface is equal to mean velocity of flow exiting between the swabs. When b/a = 2.0 peak tangential velocity drops 0.36 v_0 as shown by results in **Figure 15**. Thus to obtain a peak tangential velocity of 1.5 inches/ sec in a 14-inch well with a 7-inch filter pack (k_1 = 10,000 gpd/ft^2)

$$Q = 1.5 \text{ cfs} = 666 \text{ gpm}$$

The pressure difference necessary to produce this flow is

$$H = \frac{Q}{4\pi B_0 k_1} \quad \text{with } B_0 = 0.76 \qquad \text{(see Appendix A)}$$

$$= 17.4 \text{ ft.}$$

For the actual case considered above with a flow of 2200 gpm and a swab bypass then, from **Figure 16**, with a b/a = 1.67 and a 5-foot swab spacing (L/a = 3.33), peak tangential velocity is predicted to be 0.55 ft/ sec. For b/a = 1.67 and L/a = 1.0 (18-inch swab spacing) tangential velocity is 0.45 ft/ sec. The slight reduction that is predicted in the peak tangential flushing velocity at the formation/ filter pack interface is a consequence of a less uniform flow distribution in the filter pack as the swabs are moved closer together (Section 2.5).

With a double swab the effect of undersized swabs on clearance must be compensated by increasing pump capacity to offset leakage past the swabs. As discussed in Section 3.2, the effect of providing flange clearance is the same as introducing an orifice that permits flow to bypass the swab. With a ¼-inch clearance on the swab diameter in a 14-inch diameter well it was estimated that 10 ft of head would produce a flow of about 600 gpm. Thus with two flanges an extra 1200 gpm is required. Adding this to the 666 gpm required for flushing the gravel gives a total of about 1900 gpm.

3.6 Performance Summary

We can summarize the previous discussion of the various methods in terms of the tangential velocities induced at the filter pack/ formation interface to develop a typical 14-inch diameter well with 28-inch diameter filter pack.

Method	**Injection Flow Required**	**Peak Tangential Velocity at the bore hole**
Jetting (3 jets)	312 gpm	0.003 ft/ sec
Line Swab (10 ft of water above swab)	----	0.125 ft/ sec transient
Rocker Beam (10 ft of water above swab)	----	0.125 ft/ sec pulsating
Single Swab with Injection	180* gpm minimum	0.125 ft/ sec
Falling Single Swab with Injection	180* gpm minimum	very high
Double Swab no Bypass with Injection	180* gpm minimum	0.125 ft/ sec
Double Swab with Bypass with Injection	666 gpm	0.125 ft/ sec

* Assumes no loss to recharge

3.7 Conclusions

The preceding analysis and computations permit some conclusions to be drawn regarding the efficacy of the five well development techniques. These are:

1. Unless filter pack material is carefully chosen to provide some, but not excessive, loss through the well screen, high velocity jetting, even when considered under the most favorable assumptions, is unlikely to provide effective well development. Without some loss of particles to allow jet-induced motion of the pack material, the rate of velocity decay of the jet within the filter pack is extremely rapid. However, jetting can be an effective development technique provided motion of the filter pack is induced.
2. Line swabbing provides relatively high tangential velocities at the interface between the filter pack and the formation. At any given location the velocities occur briefly during passage of the swab. Radial production flows out of the formation, in addition to tangential scouring velocities, are developed. The magnitude of the production flow is inversely proportional to the depth of screen below the swab. For these reasons many passes of the swab are likely to be necessary to develop the well.
3. Rocker beam swabbing effectiveness is limited by the head available to produce flow through the filter pack. This may be compensated for by the pulsating flow induced. The rocking mode, combined with slow hauling, is an effective method provided that sufficient power is available to encourage transport through the filter pack.

4. Single swab development with injection pumping below the swab produces significant tangential velocities at the filter pack/ formation interface. Since the entire well is under pressure which creates recharge flows, makeup water is required. Hauling and dropping the drill pipe induces high tangential velocities in the filter pack. It is not obvious ho this flow will be divided between recharging the formation and flushing the filter pack.
5. Operation of double swab injection development depends markedly on whether a bypass conduit is available to permit return flow from below the swabs. Without this bypass the operation is virtually identical to a single swab, and flow losses to recharge may be significant from pressurization of the lower well section. With flow bypass the following comments are made:

    (i) Efficiency is high since, depending on well depth, a reasonable fraction of energy expended is within the filter pack.
    (ii) Tangential velocities within the filter pack can be controlled easily by adjusting pumping rates.
    (iii) Leakage past swab clearances can be offset by increased pumping rates to maintain the same flow through the filter pack.

4.0 REFERENCES

- Abramowitz, M. and Stegun, I.A. **Handbook of Mathematical Functions**. Dover Publications, New York, 1965.
- Bear, J. **Hydraulics of Groundwater**. McGraw-Hill, New York, 1979.
- Carslaw, H.S. and Jeager, J.C. **Conduction of Heat in Solids**. Oxford, London, 1959.
- Zdener, F.F. and Allred, R.E. "**Correct methods are essential in well development**." The Johnson Driller's Journal, January-February, 1979.

Appendix A

Mathematical Models for Development Methods

All the mathematical models are based on the well-known potential theory of flow in porous media. The basic equation for the velocity potential $\phi(r, z, t)$ is

$$\kappa\left(\frac{\partial^2\phi}{\partial z^2}+\frac{1\partial\phi}{r\partial r}+\frac{\partial^2\phi}{\partial r^2}\right)=\frac{\partial\phi}{\partial t}, \qquad (1)$$

where the velocity in the z-direction is

$$v_z = -k \frac{\partial \phi}{\partial z} \qquad (2)$$

and in the radial direction

$$v_r = -k \frac{\partial \phi}{\partial z} \qquad (3)$$

k is the hydraulic conductivity, κ = k/S where S is the specific storativity for the medium, In general, S is small (10^{-4} - 10^{-6}). For steady flow $\partial\phi / \partial t = 0$, and we have

$$\frac{\partial^2 \phi}{\partial z^2} + \frac{1 \partial \phi}{r \partial r} + \frac{\partial^2 \phi}{\partial r^2} = 0.$$

For layered media we have two such potential functions ϕ_1 and ϕ_2, and these satisfy conditions

$$\phi_1 = \phi_2, k_1 \frac{\partial \phi 1}{\partial n} = k_2 \frac{\partial \phi 2}{\partial n} \qquad (5)$$

where n is the normal direction to the interface between region 1 and region 2. We consider each problem in turn.

Jetting

For steady jet flow we take coordinates (r, z) with r = 0, the axis of the jet; z = 0, the surface of the filter pack; z = T, the filter pack/ formation interface. It can be shown that

$$\phi_1(r, z) = \int_0^\infty f(\lambda) J_0(\lambda r)_1 \left[\frac{k_1 \cosh \lambda (t - z) + k_{2 \sinh \lambda (T - z)}}{k_1 \cosh \lambda T + k_2 \sinh \lambda T} \right] d\lambda \qquad (6)$$

and $\phi_2(r, z) = \int_0^\infty f_2(\lambda) J_0(\lambda r) e^{-1 12 z} d\lambda$

satisfy the differential equation (4) and (5). The solution then requires finding $f_1(\lambda)$ such that

$$\phi_1(r, o) = 0 \qquad \text{for } r > c \qquad (7)$$

$$2\pi \int_0^c k_1 \frac{\partial \phi 1}{\partial z} r dr = Q \qquad (8)$$

Condition (7) specifies a constant potential surface outside the jet; condition (8) that the jet flow into the medium is correct. The correct function $f(\lambda)_1$ is found by analogy with a homogeneous medium heat flow problem given in Carslaw and Jaeger (1959), page 217. It is

$$f(\lambda)_1 = \frac{Q}{2\pi c k_1 A\lambda}\left(\frac{\sin\lambda c}{\lambda c}\cos\lambda c\right) \qquad (9)$$

where

$$A = \int_0^\infty \frac{J_1(t)}{t}\left(\frac{\sin t}{t} - \cos t\right)\tanh\left(\frac{tT}{c} + \in\right) dt \qquad (10)$$

In these formulae J_0 and J_1 are Bessel functions of order 0 and 1 and

$$\in = \tfrac{1}{2}\log_e\left(\frac{1 + k_2/k_1}{1 - k_2/k_1}\right) \qquad (11)$$

From formulae (6), (9) and (10) and formulae (2) and (3) it is possible to evaluate the velocities in the filter pack. The integrals were computed using polynomial approximations for J_0 (x) and J1 (x), (Abramowitz and Stegun [1965], page 370, and Simpson's 3/8-rule numerical integration formula A&S, page 886). A step length of 0.01 appeared adequate with all computations performed in double-precision arithmetic (17 significant figures). Evaluation of formulae (10) gave a value of A = 0.7648 for T/c = 28 and $\in$ = 0.001, and integrating to t = 750. This agrees reasonably well with the maximum possible value for the integral, which occurs when T/c is very large, and the integral can be evaluated exactly to give π /4 = 0.7854. The integrals for velocity converge very quickly on z = T due to the presence of a cosh $\left(\lambda\frac{T}{c} + \in\right)$ term in the denominator.

Swabbing

For the swabbing problems coordinates were taken with z on the axis of the well and r radially from the well axis, so that the well screen was r = a and the filter pack/ formation interface, r = b.

The moving swab problem was solved by changing to coordinates moving with the swab to give a general solution for ϕ_1 that satisfies conditions (5) and equation (4) plus a term $-U\partial\phi/\partial z$. Since the solution must be odd in z, and the eigenfunctions of the equation are sin λz, cos λz and I_0 (ξ r), K_0 (ξ r) where $\xi = (\lambda^2 + U/2\kappa)$,½ and I_0 and K_0 are modified Bessel functions of the first and second kind, the general solutions for ϕ_1 is

$$\phi_1(r,z) = e^{\frac{\gamma z}{a}}\int_0^\infty f(t)sn(t\frac{z}{a}\left[\frac{\alpha I_0(\xi\frac{r}{a}) + \beta K_0(\xi\frac{r}{a})}{\alpha I_0(\xi) + \beta K_0(\xi)}\right] dt \qquad (12)$$

where:

$\xi = (t^2 + \gamma^2)^{\frac{1}{2}}$

γ = aU/2κ

$\alpha = 1 - k_2/k_1$

$\beta = I_1(\xi\frac{b}{a})/K_1(\xi\frac{b}{a}) + (k_2/k_1)I_0(\xi\frac{b}{a})/K_0(\xi\frac{b}{a})$

and I_1 and K_1 are modified Bessel functions of order 1. $f(t)$ must be chosen so that

$\phi_1 = \begin{cases} +H/2 & \text{on } z > 0, r = a \\ -H/2 & \text{on } z > 0, r = a \end{cases}$ and

This is achieved by choosing

$$f(t) = \frac{Ht}{\pi(t^2 + \gamma^2)}$$

Although this expression appears somewhat formidable the velocities can be evaluated using formulae (2) and (3). Numerical integration is performed as before using polynomial approximations for the modified Bessel functions. The results for v_t are given in **Figure 13** for the case γ = 0.1. For γ = 0.001, the results appear independent of γ and agree identically with the results of a steady swab calculation to be described below.

The solution for ϕ_2 has not been evaluated numerically but must be of the form

$$\int_0^\infty f_2(t)\sin(t\frac{z}{a})K_0(\xi\frac{r}{a})dt,$$

since it is known that $\phi_2 \to 0$ as r becomes large.

Rocker Beam Swabbing

In the previous case where there is a steady velocity a simple change in coordinates was sufficient to enable a solution. Here, the solution will be of the form

$$\phi(r,z,t) = \mathrm{Re}\left[e^{i\omega t}\psi(r,z)\right],$$

where Re stands for the real part and $i = \sqrt{-1}$, $\omega = 2\pi f$ where f is the stroking frequency of the oscillation. For this problem the equation is formula (1).

The solution for ϕ_1 in this case is given by

$$\phi_1(r,z,t) = \frac{2H}{\pi}\mathrm{Re}\left\{e^{i\omega t}\int_0^\infty \frac{J_0(l\lambda)\sin\lambda z}{\lambda}\left[\frac{\alpha I_0(\xi r) + \beta K_0(\xi r)}{\alpha I_0(\xi a) + \beta K_0(\xi r)}\right]dt\right.$$

with α and β as before but with

$$\xi = (\lambda^2 + i\omega/\kappa)^{1/2}$$

and l = length of swab stroke.

Evaluation of this would be very time consuming, and it is fortunate that ω / κ is very small. The solution can therefore be approximated closely by putting $\xi = \lambda$ in the integral above. The solution is then a function of the ratio of l / a. However, evaluation of v_t/v^* at z = 0 for l / a = 0.1 gives a value of 3.01 and for l / a = 0.01 a value of 3.01. It seems reasonable to conclude that for l / a small the solution is identical with that found as for the line hauling swab (a satisfying check!). In other words, the oscillatory solution is a succession of steady state solutions since the medium responds faster than the period of oscillation. The numerical computations for v_t/v^* at r = b are given in **Figure 14**.

Injection Swabbing

For this case the flow is steady so the equation is (4) and the boundary conditions at r = a are that ϕ_1 for |z|>2L and

$$-2\pi a \int_0^L k_1 \frac{\partial \phi 1}{\partial r} dz = Q$$

with condition (5) at r = b. The solution to this problem is given by

$$\phi_1(r,z) = \frac{Q}{4\pi a B_0} \int_0^\infty \frac{J_1(L\xi)\cos z\xi}{\xi} \left[\frac{\alpha I_0(\xi r) + \beta K_0(\xi r)}{\alpha I_0(\xi a + \beta K_0(\xi a)} \right] d\xi ,$$

where α and β are as previously and

$$\beta_0 = \int_0^\infty \frac{J_1(t\frac{L}{a})\sin(t\frac{L}{a})}{t} \left[\frac{\alpha I_1(t) - \beta K_1(t)}{\alpha I_0(t) + \beta K_0(t)} \right] dt$$

The following values have been found for β_0 for b/a = 1.5, and k_2/k_1 = 0.001:

L/a	0.5	1.0	2.0
B0	0.913	0.760	0.573

For k_2/k_1 = 0.1, L/a = 1.0, b/a = 1.5, the value of B_0 changes to 0.844, thus is not very sensitive to the ratio of hydraulic conductivities. For b/a = 2.0, and k_2/k_1 = 0.001 the value of B_0 = 1.001.

Numerically computed results for the tangential velocity for the cases L/a = 1 and b/a = 1.5 and 2.0 are given in **Figures 15** and **16**. The streamline patterns are not computed but are schematic based on an evaluation of the ration of v_t/v^* at the exterior of the gravel pack.

The flow exterior to the gravel pack in the formation was not evaluated numerically. ϕ_2 is of the form

$$C\int_0^\infty \frac{J_1(L\xi)\cos 9z\xi)}{\xi} K_0(\xi r)d\xi,$$

where C is obtained by matching to ϕ_1 according to formula (5).

Appendix B

Details of Jetting Model Pack Materials

The 6 14 filter pack is a mechanically graded gravel produced by Crystal Silica Co. Typical analysis:

U.S Sieve Size	% Passing
6	0
8	30
10	40
12	22
14	6

The filter pack is a mechanically graded gravel produced by Monterey Sand and Gravel. 100% passes ¼" or No. 3 U.S. Sieve, and 100% is retained on 1/8" screen. Typical analysis:

U.S Sieve Size	% Passing
3	100
4	18
6	2
8	0

The 6 10 filter pack is a mechanically graded smooth and rounded gravel. Typical analysis,

U.S Sieve Size	% Passing
4	10.0
6	95
8	18
10	1
16	0